A mechatronic power boosting design for piezoelectric generators

Haili Liu, Junrui Liang,[a] and Cong Ge
School of Information Science and Technology, ShanghaiTech University, No. 8 Building, 319 Yueyang Road, Shanghai 200031, China

(Received 4 August 2015; accepted 23 September 2015; published online 5 October 2015)

It was shown that the piezoelectric power generation can be boosted by using the synchronized switch power conditioning circuits. This letter reports a self-powered and self-sensing mechatronic design in substitute of the auxiliary electronics towards a compact and universal synchronized switch solution. The design criteria are derived based on the conceptual waveforms and a two-degree-of-freedom analytical model. Experimental result shows that, compared to the standard bridge rectifier interface, the mechatronic design leads to an extra 111% increase of generated power from the prototyped piezoelectric generator under the same deflection magnitude excitation. The proposed design has introduced a valuable physical insight of electromechanical synergy towards the improvement of piezoelectric power generation. © *2015 AIP Publishing LLC*.
[http://dx.doi.org/10.1063/1.4932519]

Vibration is one of the most promising ambient energy sources, which can be exploited for powering the dispersive wireless sensor networks (WSNs).[1,2] Due to the unique features of the piezoelectric generators (PGs), such as high output voltage, easy to be integrated, and high energy density, they are very suitable for constructing compact vibration energy harvesting systems. Therefore, the PGs have attracted extensive research effort during the last decade.[3–5]

Given the capacitive nature of PGs, their energy harvesting capability can be increased by several hundred percent by connecting themselves to some power conditioning circuits, such as the synchronized switch harvesting on inductor (SSHI)[6] and other synchronized switch interface circuits.[7] In SSHI, the power conditioning circuit detects the maximum deforming instants of a PG, and simultaneously forms an inductive shortcut for the charge stored in the PG, such that the voltage across the piezoelectric element can be inverted after half of an RLC cycle. In order to carry out these sensing and switching actions without extra power effort, some self-powered solutions have been invented,[8–11] which make SSHI more applicable for engineering practice. In these solutions, the synchronized switch actions are carried out by three functional blocks, i.e., voltage peak detector, comparator, and electronic switch. The non-idealities of practical building blocks lead to some side-effects.[9,12] For example, in the bipolar junction transistor (BJT) solutions,[8,9] the open circuit voltage of the PG is lowered by the non-ideal peak detector; a switching delay is introduced by the non-ideal comparator; a large threshold voltage is set by the non-ideal switch. These side-effects discount the original improvement.[9,13] On the other hand, in the metal oxide semiconductor (MOS) solutions, due to the voltage constraint of most integrated MOS transistors, the manageable peak-to-peak voltage of the PG is usually observed to be lower than 10 V.[10,11]

Regarding the aforementioned limitations of the previous electronic solutions, this letter proposes a mechatronic self-powered SSHI (MSP-SSHI) solution, which is more compact and more universal for the operation under a wide range of vibration level. The configuration and working principle of the MSP-SSHI based PG are shown in Fig. 1. The key component of this design is a low-cost vibration sensing switch (VSS). The compact VSS can be used for detecting the vibration phase and simultaneously carrying out switching actions; therefore, it is a good substitute of the auxiliary electronic blocks in the self-powered SSHI. As shown in Fig. 1, the VSS is composed of a soft cantilever and a framework fixed at the free end of the piezoelectric cantilever. Three electrodes are installed in the VSS: one at the moving cantilever as a single pole and two at the VSS framework as double throws. When subjected to vibration, the moving pole will alternatively hit the two throws. By properly connecting the three electrodes to an inductive rectifier circuit, as shown in Fig. 1, the SSHI function can be realized with this electromechanical synergy.

Figs. 1(a) and 1(b) show the two synchronized instants, when the moving pole hits the two stationary throws,

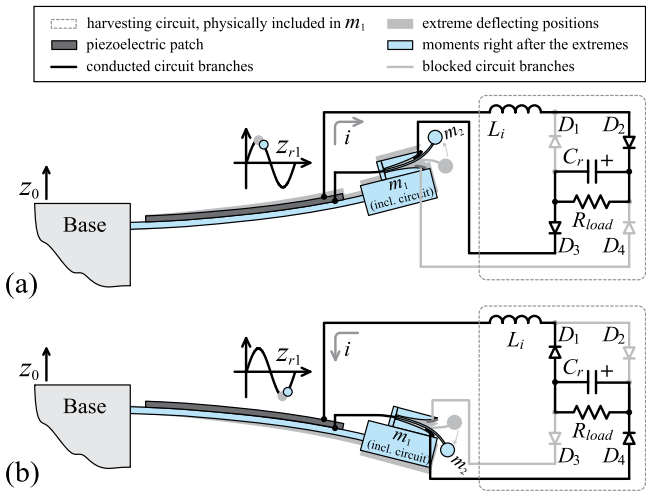

FIG. 1. The working principle of MSP-SSHI. (a) Synchronized instants right after the maximum contraction; (b) after the maximum extension.

[a]Electronic mail: liangjr@shanghaitech.edu.cn

respectively. In Fig. 1(a), the piezoelectric patch has just experienced its maximum contraction (grey trail) and starts to stretch. At this moment, the moving pole is released from the lower throw and hits the upper throw because of its moving inertia. The new connection enables the current flow through the highlighted circuit branch, which forms an RLC resonance for instantaneous voltage inversion. In the circuit, the diode D_3 is used for blocking the reverse current flow from the inductor. Therefore, once the voltage is inverted, it will not rewind. Fig. 1(b) shows the opposite position of that in Fig. 1(a) after the piezoelectric patch reaches its maximum extension (grey trail). The moving pole leaves the upper throw and hits the lower, which enables the voltage inversion in the other direction. As the moving direction of the piezoelectric cantilever can be identified by the mechanical VSS, no active transistor is required for the self-powered control; therefore, compared to the previous design,[9] the number of diodes that used for rectification can be also reduced. By decreasing the forward voltage drop in rectification (only two diode drops in this design), the diode loss can be eliminated.

The dynamic analysis of the mechanical VSS and piezoelectric cantilever combination can be started from a boundless two degree-of-freedom (2DOF) model, as shown in Fig. 2(b). The main vibrator, which is composed of equivalent mass m_1, effective stiffness k_1, and damping coefficient d_1, models the first flexural mode of the piezoelectric cantilever;[14] the auxiliary vibrator, which is composed of m_2, k_2, and d_2, gives a linear approximation of the VSS moving pole. In Fig. 2(b), z_0 is the base movement; z_1 and z_2 are the absolute displacements of m_1 and m_2, respectively; z_{r1} is the relative displacement of m_1 with respect to the base, which is proportional to the deflection of the piezoelectric cantilever; z_{r2} is the relative displacement of m_2 with respect to m_1, which indicates the distance between the pole and throws in the VSS. The relation between z_{r1} and z_{r2} indicates whether the switch can be conducted in time when the piezoelectric cantilever reaches its deflecting extremes.

Defining $\tilde{m} = m_2/m_1$ as the mass ratio; $\omega_j = \sqrt{k_j/m_j}$, where $j = 1$ or 2, as the resonant frequencies of the vibrators; $\zeta_j = d_j/(2m_j\omega_j)$ as their damping ratios, respectively, the equation of motion of the 2DOF system can be expressed as follows:

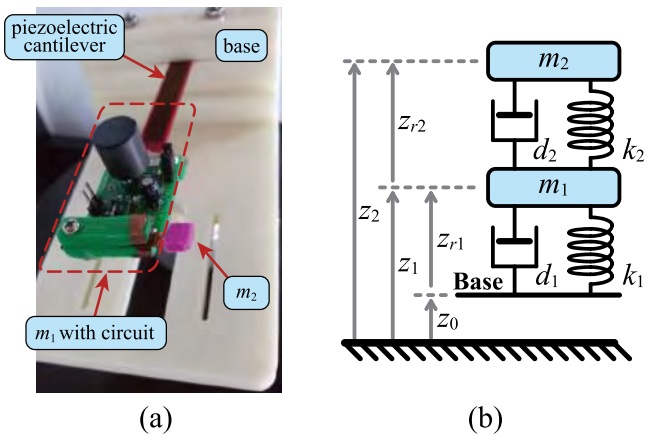

FIG. 2. (a) Practical implementation of MSP-SSHI. (b) 2DOF linear model for the system.

$$\ddot{z}_{r1} + 2\omega_1\zeta_1\dot{z}_{r1} + \omega_1^2 z_{r1} - \tilde{m}[2\omega_2\zeta_2\dot{z}_{r2} + \omega_2^2 z_{r2}] = -\ddot{z}_0, \quad (1)$$

$$\ddot{z}_{r2} + 2\omega_2\zeta_2\dot{z}_{r2} + \omega_2^2 z_{r2} = -\ddot{z}_1. \quad (2)$$

From (1) and (2), the relation of z_{r1} and z_{r2} can be obtained in the frequency domain as follows:

$$\frac{Z_{r2}}{Z_{r1}} = \frac{2\omega_1\zeta_1 s + \omega_1^2}{\left(s^2 + 2\omega_2\zeta_2 s + \omega_2^2\right) + \tilde{m}\left(2\omega_2\zeta_2 s + \omega_2^2\right)}, \quad (3)$$

where $s = j\omega$, and ω is the excitation angular frequency. When the system vibrates under the resonant frequency ω_1, i.e., $\omega = \omega_1$, (3) can be simplified into

$$\frac{Z_{r2}}{Z_{r1}} = \frac{1 + 2j\zeta_1}{(1+\tilde{m})\tilde{\omega}(\tilde{\omega} + 2j\zeta_2) - 1}, \quad (4)$$

where $\tilde{\omega} = \omega_2/\omega_1$ is defined as the frequency ratio. In addition, if we can intentionally design $\tilde{\omega} \ll 1$, $\tilde{m} \ll 1$, $\zeta_1 \ll 1$, and $\zeta_2 \ll 1$, (4) can be further simplified into

$$\frac{Z_{r2}}{Z_{r1}} = -1. \quad (5)$$

The derivation from (3) to (5) indicates that the relative movement of the piezoelectric cantilever and that of the VSS can be totally out of phase when several parametric and operational conditions are satisfied. These criteria lead to five design rules for the MSP-SSHI based PG, which are listed as follows:

- The resonant frequency of the VSS should be much lower than that of the main piezoelectric cantilever.
- The moving mass of the VSS should be much smaller than the equivalent mass of the main cantilever, such that the installation of the VSS can hardly affect the dynamics of the piezoelectric cantilever.
- The VSS moving part should be a low-loss structure.
- The main piezoelectric cantilever should be a low-loss cantilever. This condition coincides with the cantilever design for energy harvesting purpose.
- The whole system operates near the resonant frequency of the main piezoelectric cantilever.

Under the aforementioned conditions, the out-of-phase relation between z_{r1} and z_{r2}, as, respectively, shown by the dotted line and dashed line in Fig. 3, is obtained by assuming that the relative movement of m_2 is boundless. Nevertheless, in a real VSS, the relative movement of m_2, i.e., z_{r2}, is bounded in both directions. The two boundaries, shown by grey dashed dotted lines in Fig. 3, reset the z_{r2} waveform. Ideally, without strong collision, the VSS beam adheres at either of the boundaries most of the time in a cycle; while in the transitional intervals, usually right after the maximum deflecting places of the main cantilever, the moving pole leaves from one boundary, follows the moving trend of boundless z_{r2}, until it hits the throw on the other side. The solid line in Fig. 3 shows the conceptual waveform of z_{r2} under the bounded condition. The bounded z_{r2} has an approximately 90° phase difference compared to z_{r1}. It means that the moving pole of the VSS changes its contacting throw once z_{r1} attains an extreme value, i.e., at the maximum

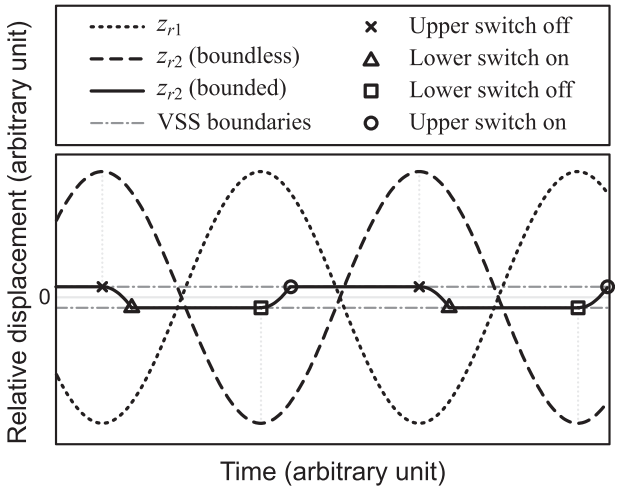

FIG. 3. Conceptual displacement waveforms.

contraction and extension instants of the piezoelectric element. Based on this principle, the VSS can be used to generate synchronized switch actions for the SSHI purpose.

The MSP-SSHI based PG has been practically implemented, as shown in Fig. 2(a). The piezoelectric cantilever (effective dimension $50.00 \times 8.10 \times 0.95\,\text{mm}^3$) is built with a commercial piezoelectric bimorph (material: PZT-5H; d_{31}: -440 pm/V; model: QDTE52; manufacturer: Pant Piezoelectric Tech. Co., Ltd, Suzhou, China). One of the piezoelectric patch is used for energy harvesting purpose, while the other is used as the reference of beam deformation, i.e., z_{r1}. The fixed end of the piezoelectric cantilever is excited by a shaker near its resonant frequency, 29.8 Hz. The mechatronic power booster including the VSS and inductive rectifier circuit is installed at the free end of the cantilever. The soft moving pole of the VSS is cut from a 0.1 mm copper sheet. In order to prevent the hard collision and multiple strikes between the pole and throw in each synchronized instant, the moving mass of the VSS, i.e., m_2, is placed outside the rigid frame, as shown in Figs. 1 and 2(a). In addition, the inner side of the VSS frame is fabricated into an arc shape for making better conducting contacts between the pole and throws, as illustrated in Fig. 1. In most of the previous SSHI designs, the bulky inductor and discrete circuit components were regarded as a burden against miniaturization.[15] In this design, we make a good use of this burden by mounting the whole circuit at the free end of the piezoelectric cantilever. On one hand, the circuit can be easily bonded to the piezoelectric electrodes for making an integrated device; on the other, the weight of all circuit components acts as the proof mass of the piezoelectric cantilever, which can lower the operating frequency and increase the vibration magnitude of the piezoelectric cantilever.

In experiment, the synchronized switching function of the MSP-SSHI is firstly tested. Fig. 4(a) shows the voltages across the two piezoelectric patches, one with MSP-SSHI and the other is open-circuited as the reference. Experimental voltage waveforms show that the VSS can catch the maximum deflecting instants and perform perfect synchronized switches in time. Because the sensing and switching function are not constrained by active transistors,

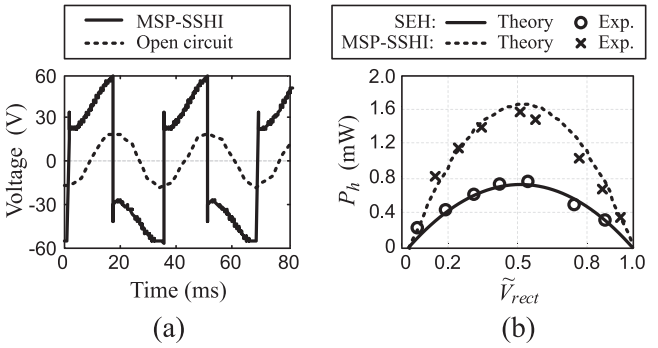

FIG. 4. Experimental results. (a) Voltage across the piezoelectric patches. (b) Harvested power with SEH and MSP-SSHI.

as the previous studies did, the manageable piezoelectric voltage can be large. As we can observe from Fig. 4(a), the peak-to-peak voltage has reached 120 V in this experimental case.

To validate the power boosting effect of the MSP-SSHI, a comparative study between the standard energy harvesting (SEH) interface (bridge rectifier) and the MSP-SSHI is further carried out. The mechanical configurations in both cases are the same. In MSP-SSHI, the switching circuit embedded in m_1 is activated. In SEH, it is deactivated, instead, an external bridge rectifier outside m_1 is connected for SEH. In experiment, the PG is excited at a constant displacement magnitude, which equivalently generates a 18.5 V peak-to-peak voltage on the reference piezoelectric patch. The harvested power under different load resistor R_{load} is recorded. Besides the experimental results, we also employ the impedance based analysis[16] for validating the correspondence between theory and experiment. Both of the theoretical and experimental harvested powers as functions of the non-dimensional rectified voltage $\tilde{V}_{rect}$ are shown in Fig. 4(b). $\tilde{V}_{rect}$ is defined as the rectified voltage V_{rect} over the open-circuited voltage V_{OC}, i.e., $\tilde{V}_{rect} = V_{rect}/V_{OC}$. The DC harvested power $P_h = V_{rect}^2/R_{load}$. From the results, maximum harvested powers of 1.536 mW and 0.729 mW are obtained for MSP-SSHI and SEH at the optimal load resistors of 60 kΩ and 140 kΩ, respectively. Therefore, by taking the MSP-SSHI solution, in substitute of the SEH, the output power of the PG has been increased by 111% in this study.

In summary, this letter has introduced a mechatronic scheme for synchronized switch power boosting in piezoelectric generator. The key component in this scheme is a mechanical VSS, which can automatically switch at maximum deflecting instants of the piezoelectric cantilever. Five designed rules have been derived based on a two degree-of-freedom model; some design tricks for the VSS and system have also been introduced. It has been shown that the MSP-SSHI solution outperforms the SEH and increases the generated power by 111% without providing any additional sensing, control, and power source. Owing to the effective electromechanical synergy, the MSP-SSHI solution is self-contained, compact, and universal for working under high piezoelectric voltage; therefore, it is a good candidate for power boosting purpose in stand-alone piezoelectric generator towards efficient ambient vibration energy harvesting.

The work described in this paper was supported by the grant from National Natural Science Foundation of China (Project No. 61401277) and the Faculty Start-up Grant of ShanghaiTech University (Project No. F-0203-13-003).

[1]Y.-J. Lai, W.-C. Li, C.-M. Lin, V. V. Felmetsger, D. G. Senesky, and A. P. Pisano, in *Technical Digest of IEEE Solid-State Sensors, Actuators and Microsystems Workshop* (2012), pp. 505–508.
[2]Y.-J. Lai, W.-C. Li, C.-M. Lin, V. Felmetsger, and A. P. Pisano, in *2013 Transducers & Eurosensors XXVII* (2013), pp. 2268–2271.
[3]A. Erturk, J. Hoffmann, and D. J. Inman, Appl. Phys. Lett. **94**, 254102 (2009).
[4]M. Lallart and D. Guyomar, Appl. Phys. Lett. **97**, 014104 (2010).
[5]L. Xie and M. Cai, Appl. Phys. Lett. **105**, 143901 (2014).
[6]D. Guyomar, A. Badel, E. Lefeuvre, and C. Richard, IEEE Trans. Ultrason., Ferroelectr., Freq. Control **52**, 584 (2005).
[7]D. Guyomar and M. Lallart, Micromachines **2**, 274 (2011).
[8]M. Lallart and D. Guyomar, Smart Mater. Struct. **17**, 035030 (2008).
[9]J. Liang and W.-H. Liao, IEEE Trans. Ind. Electron. **59**, 1950 (2012).
[10]N. Krihely and S. Ben-Yaakov, IEEE Trans. Power Electron. **26**, 612 (2011).
[11]Y. Sun, N. H. Hieu, C.-J. Jeong, and S.-G. Lee, IEEE Trans. Power Electron. **27**, 623 (2012).
[12]F. Giusa, F. Maiorca, A. Noto, C. Trigona, B. Ando, and S. Baglio, Sens. Actuators, A **212**, 34 (2014).
[13]Y. S. Shih, S. C. Lin, M. Lallart, and W. J. Wu, in *Proceedings of ASME Conference on Smart Materials, Adaptive Structures and Intelligent System* (2013), p. V002T07A005.
[14]A. Badel, M. Lagache, D. Guyomar, E. Lefeuvre, and C. Richard, J. Intell. Mater. Syst. Struct. **18**, 727 (2007).
[15]Y. Ramadass and A. Chandrakasan, IEEE J. Solid-State Circuits **45**, 189 (2010).
[16]J. Liang and W.-H. Liao, IEEE/ASME Trans. Mechatron. **17**, 1145 (2012).